ISSN: 2178-7727

Evaluation of Stress-Induced Microstructural Changes in Concrete Using Ultrasonic Pulse Velocity (UPV) with Variable Transducer Sizes

Ayush Mittal[1], Ramesh Kumar Verma[2], Shivakar Prasad[3]

[1]Assistant Professor, Dept. of Civil Engineering, REC Ambedkar Nagar, India. Email: ayushmittalce0012@gmail.com
[2]Assistant Professor, Dept. of Mechanical Engineering, Khwaja Moinuddin Chishti Language University, Lucknow, India. Email: rv2986iet@gmail.com
[3]Assistant Professor, Dept. of Mechanical Engineering, Kamla Nehru Institute of Physical and Social Sciences, Engineering Institute, Sultanpur, India. Email: shiva.jais2000@gmail.com

ABSTRACT
The Ultrasonic Pulse Velocity (UPV) test is a non-destructive method used to evaluate the structural integrity, homogeneity, and compressive strength of concrete. It is based on the principle that the propagation speed of high-frequency sound waves correlates with the elastic properties and density of the material. In this study, two transducer sizes—28 mm (150 Hz) and 49.7 mm (54 Hz)—are employed to examine the influence of sensor size on signal propagation. A transmitting transducer generates a mechanical pulse, while a receiving transducer on the opposite surface records it. The transit time is measured to calculate pulse velocity using V=L/T, where V is velocity (m/s), L is the direct path length (m), and T is travel time (s). UPV serves as a key indicator of concrete quality: higher velocities suggest sound material, whereas lower values indicate cracks, voids, or weak zones. The study explores the relationship between incremental compressive stress and UPV in 64 concrete cubes across eight mix grades (M10–M45). Specimens are divided equally between the two transducer types for direct comparison under identical conditions. After 28 days of curing, samples undergo monotonic axial loading to failure, with UPV readings recorded at each stress stage. The investigation aims to correlate pulse velocity attenuation with increasing stress, anticipating a gradual decline in UPV as compressive stress rises. Findings will enhance understanding of stress-induced microstructural changes in concrete, demonstrating UPV's capability as a sensitive, non-destructive evaluation tool for detecting internal deterioration under load.

KEYWORDS: NDT – Non-Destructive Test, UPV – Ultrasonic Pulse Velocity, Co-Factor, Compressive stress, Transducers

INTRODUCTION
Concrete is a composite material formed by blending cement, aggregates, and additives such as chemical admixtures. To evaluate the structural integrity of hardened concrete in existing structures, non-destructive testing (NDT) methods like ultrasonic pulse velocity (UPV) are employed. This technique utilizes portable equipment for rapid assessment, offering user-friendly operation and minimal structural interference [1–2]. The practice of in-situ concrete evaluation emerged in the 1930s, initially incorporating mechanical methods such as percussive chisel assessments, core extraction analyses, ballistic impact evaluations using specialized firearms, indirect tensile (Brazilian) tests, anchorage resistance pull-out measurements, strain monitoring during load application, and modified Brinell indentation protocols [3]. Among these, Brinell-based hardness testing gained prominence in European structural evaluation standards due to its procedural simplicity and efficiency [4–5]. Subsequent research over four decades adapted the Brinell method to cementitious matrices, establishing empirical relationships between surface hardness and compressive strength in mortars and concrete [6].

Ultrasonic pulse velocity testing has long served as a diagnostic tool for monitoring, setting and hardening processes in cement-based materials [7-8]. While supplementary cementitious materials like fly ash and slag are widely used to enhance mechanical performance, moderate hydration kinetics, mitigate alkali-silica reactivity, and reduce permeability, limited research exists on their influence on ultrasonic wave propagation parameters and correlations between UPV values and compressive strength [9-11]. Cement grade and curing

ISSN: 2178-7727

duration further influence the performance variability of these materials [12-13].

Technological advancements in 1952 streamlined UPV equipment design through spring mechanism optimization, enhancing operational ergonomics [14–16]. As a contemporary NDT method, UPV evaluates concrete homogeneity and estimates compressive strength by measuring longitudinal wave transit time between transducers [17–18]. Despite its utility, gaps persist in correlating UPV measurements with in-situ compressive stress distributions, necessitating further investigation [19–20]. This experimental investigation employs dual piezoelectric transducers with nominal diameters of 49.7mm and 28mm to transmit and receive ultrasonic pulses, enabling comparative evaluation of sensor-size effects on wave propagation characteristics [21]. The transducers' distinct contact areas and frequency responses are leveraged to assess measurement consistency and stress-induced signal attenuation across specimen geometries. This study addresses this need through an experimental program involving cubic specimens to examine correlations between ultrasonic pulse velocity attenuation and applied compressive stress levels during progressive loading [22–23]. By integrating insights from historical mechanical evaluation methods, contemporary UPV advancements, and unresolved challenges in stress-velocity modelling, the research aims to establish a robust empirical basis for interpreting UPV data in load-bearing concrete systems [24].

MATERIALS AND EXPERIMENTATION

The properties of concrete depend on the quality, proportion, and compatibility of its components. Below is a detailed overview of the materials used in concrete mix design

Cement

In the present work Portland pozzolana cement (PPC) is used, complying with IS: 1489-1991 standards. Cement acts as the binding agent and contributes to strength and durability. Additionally, PPC offers improved resistance to sulphate and chloride exposure, along with lower heat generation during hydration.
The physical properties of cement used is shown in Table 1.

Table 1. Physical Properties of Cement

S. No.	Property/Name of Test	Result
1.	Standard Consistency (%)	32
2.	Initial Setting Time (minutes)	40
3.	Final Setting Time (minutes)	410
4.	Fineness (Specific Surface) (m^2/kg)	324.8
	Compressive Strength (MPa)	
5.	(i) 03 days	16.9

Fine Aggregate (Coarse Sand)

Coarse sand used in the present work having fineness modulus of 3.13 and meeting the requirement of grading zone-II (IS 383) is shown in Table 2. In order to ensure denser concrete mix, sieving is performed to remove unwanted substances (organic and other foreign materials).

Table 2. Cumulative Percent Retained on various sieve sizes

S. No.	I.S. Sieve Designation	Cumulative percentage
1.	10 mm	0
	4.75 mm	9.4
	2.36 mm	23.1
	1.18 mm	40.5
	600 microns	58.9
	300 microns	82.7
	150 microns	98.4
2.	Fineness Modulus = 3.13	

ISSN: 2178-7727

Coarse Aggregate

Crushed stone or gravel with a nominal size of 20mm having fineness modulus of 7.01 is used in the study. Its angular design ensures durability and consistency in the concrete mix while providing structural strength and reducing drying shrinkage. Table 3 shows the gradation of coarse aggregate.

Table 3. Cumulative Percent Retained on various sieve sizes

S. No.	I.S. Sieve	Cumulative percentage
1.	80 mm	0
	40 mm	0
	20 mm	13.6
	10 mm	89.2
	4.75mm	98.1
	2.36 mm	100
	1.18 mm	100
	0.6 mm	100
	0.3mm	100
	0.15mm	100
2.	Fineness Modulus = 7.01	

Water

Water is essential in concrete for two main purposes. First, it acts as a key component in the chemical reaction with cement, known as hydration, which causes the concrete to harden and develop strength. Second, it serves as a lubricant, enhancing the mixture's workability and making it easier to handle and pour. Table 4 shows the obtained and permissible values of various minerals present in potable water.

Table 4. Obtained and Permissible Values of Water

S.No	Parameters	Obtained Value	Permissible Value	IS Code
1	Organic	188mg/l	200mg/l	IS 3025 (Part 18)
2	Inorganic	3114mg/l	3000mg/l	IS 3025 (Part 18)
3	Sulphates (SO_4)	365mg/l	400mg/l	IS 3025 (Part 24)
4	Chlorides (Cl)	2158mg/l	2000mg/l	IS 3025 (Part 32)
5	Suspended matter	1912mg/l	2000mg/l	IS 3025 (Part 17)

Figure 1(a), 1(b) and 1(c) shows the cement, fine and coarse aggregate samples used in the present study.

Fig. 1. (a) Cement (b) Fine aggregate (c) Coarse Aggregate

Composition of Concrete

The concrete mix proportions for grades M10 to M45, as detailed in Table 5, demonstrate a systematic variation in component ratios to achieve targeted compressive strengths and material efficiency.

ISSN: 2178-7727

Table 5. Concrete Composition for Grades M10 to M45

Grade	Cement (g)	Fine Aggregate (g)	Coarse Aggregate (g)	Water (g)	w/c Ratio	Density (kg/m³)	Comp. Strength (MPa)
M10	743–810	2025–2194	4219–4556	445–489	0.60–0.65	2300–2350	10
M15	1013–1080	1856–2025	3881–4219	557–591	0.55–0.60	2350–2400	15
M20	1283-1350	1856–2025	3713–4050	642–675	0.50–0.55	2400–2450	20
M25	1485-1553	2025–2194	3544–3881	668–709	0.45–0.50	2420–2470	25
M30	1688-1755	1688–1856	4050–4219	642–675	0.38–0.42	2450–2500	30
M35	1823–1890	1755–1924	3544–3881	642–675	0.35–0.40	2450–2500	35
M40	2025–2093	1519–1688	3881–4050	648–675	0.32–0.35	2450–2520	40
M45	2160–2228	1451–1620	3713–3881	658–692	0.30–0.33	2450–2520	45

Specification of UPV Transducers

Direct mode of transmission was adopted to measure ultrasonic pulse velocities as this mode provides maximum energy. Two transducers having diameters 49.7mm and 28mm with frequency of 54kHz and 150 kHz respectively were used. Table 6 shows the transducers specifications used in the study.

Table 6. Ultrasonic Pulse Velocity (UPV) Transducers Specifications

Parameter	Transducer 1	Transducer 2
Type	Single-Crystal	Single-Crystal
Frequency	150 kHz ± 10 kHz	54 kHz ± 5 kHz
Bandwidth	<10 kHz	<10 kHz
Driving Voltage	-1000 V to +1000 V	-1000 V to +1000 V
Dimensions	- Diameter: 28 mm	- Diameter: 49.7 mm
	- Length (without BNC): 46 mm	- Length (without BNC): 46 mm
	- Length (with BNC): 58 mm	- Length (with BNC): 58 mm

ISSN: 2178-7727

Measurement of UPV

To investigate the relationship between UPV and compressive strength, concrete samples (150 mm cubes) are subjected to incremental compressive loads using a servo-controlled testing machine [25]. Prior to failure, UPV measurements are taken at predefined stress intervals (e.g., 5,10,15….55 N/mm^2) by placing 28 mm or 49.7 mm diameter transducers on opposing faces of the specimen in direct transmission mode as shown in Figure 2. It is measured by an ultrasonic tester model no. PL02-006-0373 B0. The larger 49.7 mm transducers (contact surface: 36.77 mm) improve coupling stability on uneven surfaces, while the compact 28 mm variants (contact surface: 22.27 mm) are suited for confined geometries [21]. A couplant ensures acoustic contact, and the pulse travel time is recorded to calculate velocity (V=L/T, where L is path length). As stress increases, UPV declines sharply due to micro-cracks thus disrupting wave transmission [26-27]. This inverse correlation between UPV reduction and crack development provides insights into damage accumulation, enabling non-

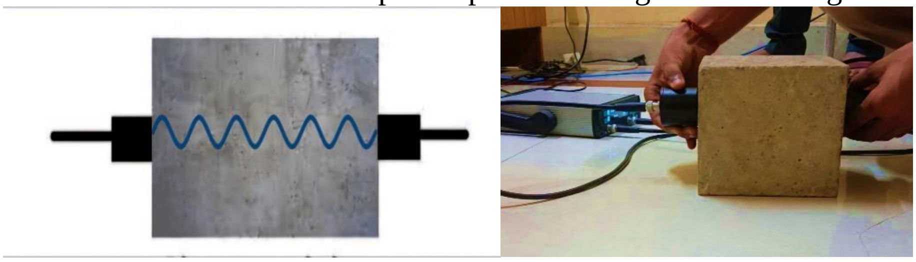

destructive prediction of residual strength and structural health monitoring under progressive loading.

Fig. 2. Positions of transducers

OBSERVATIONS AND RESULTS

Based on the tests performed, an inverse relationship between mono-axial compressive stress and ultrasonic pulse velocity (UPV) was reported [28]. As the applied compressive stress increased, the measured UPV exhibited a consistent and noticeable decline. To generalize these findings for broader applicability across different structural components, stress (rather than load or force) was selected as the key parameter for analysis. A velocity-stress graph was plotted to visualize this correlation, which confirmed that increasing stress levels significantly reduces UPV values [25]. This trend suggests that material integrity, micro-crack formation, or internal structural changes under compression influences wave propagation speed. The results highlight the sensitivity of UPV to stress variations, making it a useful indicator for assessing mechanical behaviour of concrete under compressive loading conditions [18]. Table 7 to Table 14 shows the UPV values corresponding to predefined stress on different grades of concrete having transducers of diameter 28mm and 49.7mm. Figure 3 to Figure 18 shows the velocity – stress graphs for different grades of concrete.

Table 7. Values of UPV corresponding to M10 concrete

Stress (N/mm^2)	Velocity (km/s)							
	Transducer-1 (28mm dia)				Transducer-2 (49.7mm dia)			
	Cube 1	Cube 2	Cube 3	Cube 4	Cube 1	Cube 2	Cube 3	Cube 4
5	3.058	3.013	3.079	3.109	4.189	4.167	4.275	4.191
10	2.663	2.851	2.502	2.964	3.842	3.851	4.051	3.948
15	2.297	2.661	2.327	2.734	3.635	3.588	3.854	3.614
20	2.203	2.163	2.19	2.325	3.345	3.046	3.416	2.746
25	1.533	1.636	-	1.752	2.416	2.243	2.689	2.178
30	-	0.803	-	0.989	-	-	1.748	1.6

ISSN: 2178-7727

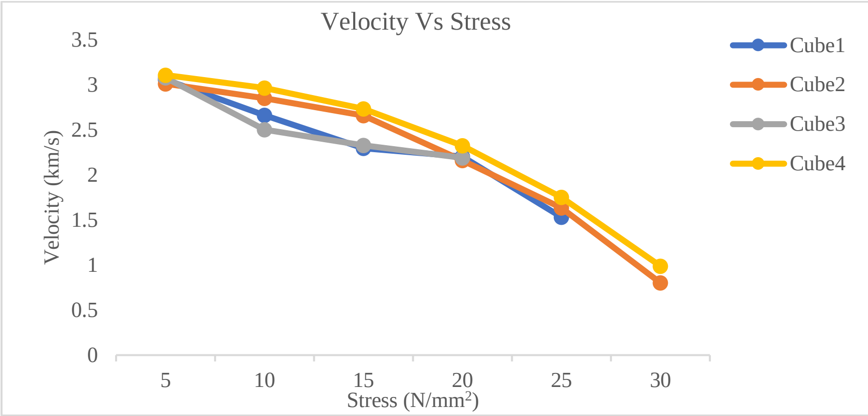

Fig. 3. Velocity versus stress graph of M10, measured using Transducer-1

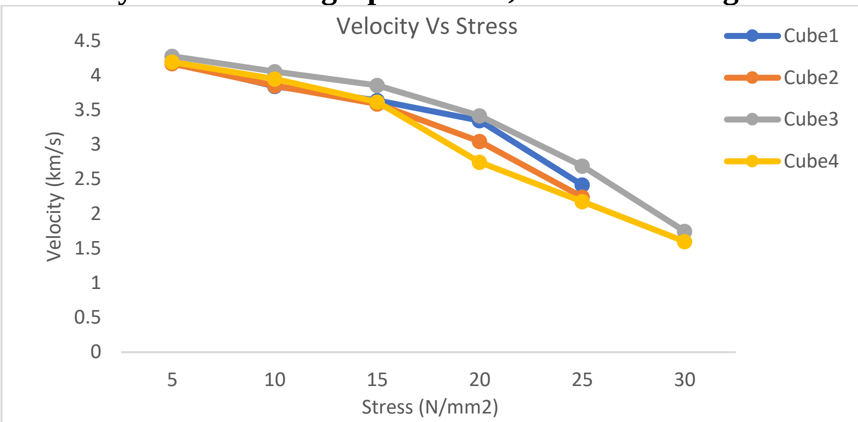

Fig. 4. Velocity versus stress graph of M20, measured using Transducer-2

Table 8. Values of UPV corresponding to M15 concrete

Stress (N/mm^2)	Velocity (km/s)							
	Transducer-1 (28 mm dia)				Transducer-2 (49.7 mm dia)			
Stress	Cube 1	Cube 2	Cube 3	Cube 4	Cube 1	Cube 2	Cube 3	Cube 4
5	3.008	3.035	3	3.072	4.256	4.083	4.254	4.289
10	2.891	2.845	2.829	2.886	3.854	3.673	3.958	3.981
15	2.814	2.706	2.6	2.655	3.514	3.371	3.542	3.546
20	2.524	2.658	2.491	2.373	3.128	2.546	3.145	3.108
25	1.792	2.2	1.657	1.982	2.546	2	3.078	2.981
30	1.022	1.47	-	1.572	1.849	-	2.41	2.845
35	-	0.868	-	1.50	-	-	1.57	-

ISSN: 2178-7727

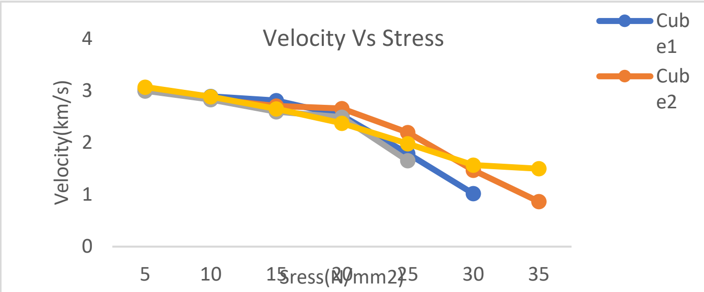

Fig. 5. Velocity versus stress graph of M15, measured using Transducer-1

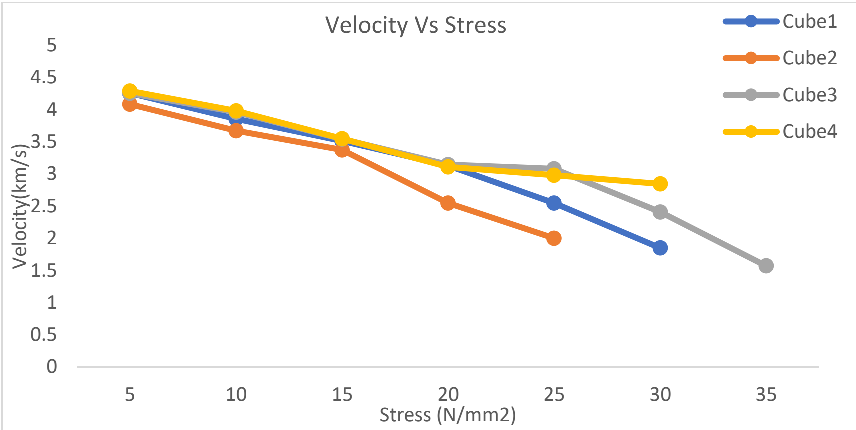

Fig. 6. Velocity versus stress graph of M15, measured using Transducer-2

Table 9. Values of UPV corresponding to M20

Stress (N/mm^2)	Velocity (km/s)							
Transducer-1 (28mm dia)					Transducer-2 (49.7mm dia)			
Stress	Cube 1	Cube 2	Cube 3	Cube 4	Cube 1	Cube 2	Cube 3	cube 4
5	3.033	2.902	3.002	3.071	4.362	4.44	4.356	4.298
10	3.0164	2.812	3.181	3.055	4.205	4.149	4.036	4.188
15	2.940	2.7083	2.961	2.895	3.956	3.873	3.852	4.021
20	2.829	2.61	2.782	2.702	3.8	3.5	3.458	4.039
25	2.505	2.464	1.808	2.541	3.698	3	2.859	3.975
30	2.054	2.095	1.655	2.256	3.423	2.243	2.008	3.851
35	1.638	1.463	1.321	1.720	3.231	1.654	1.752	3.617

ISSN: 2178-7727

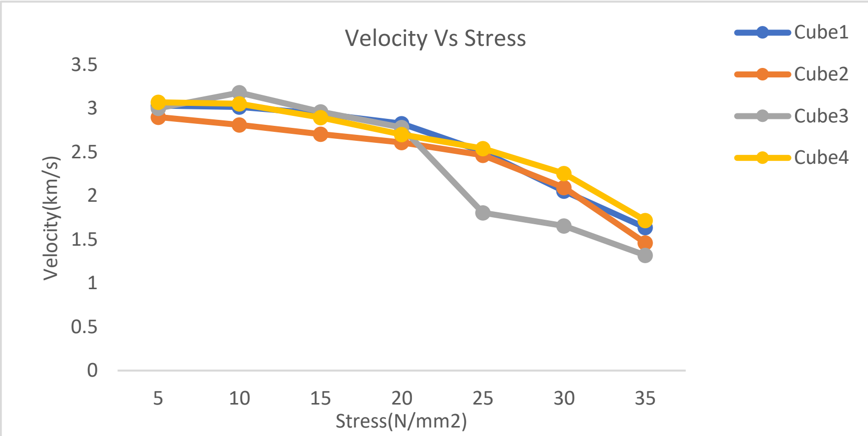

Fig. 7. Velocity versus stress graph of M20, measured using Transducer-1

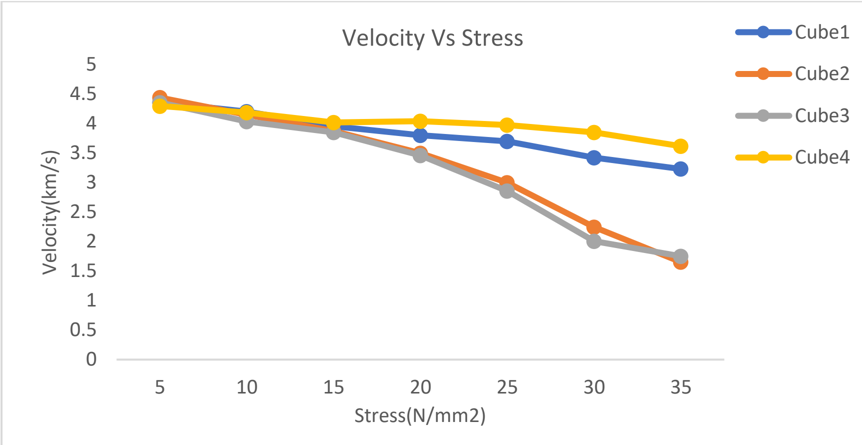

Fig. 8. Velocity versus stress graph of M20, measured using Transducer-2

Table 10. Values of UPV corresponding to M25 concrete

Stress(N/mm^2)	Velocity (km/s)							
	Transducer-1 (28mm dia)				Transducer-2 (49.7mm dia)			
Stress	Cube 1	Cube 2	Cube 3	Cube 4	Cube 1	Cube 2	Cube 3	Cube 4
5	3.120	3.075	3.151	2.978	4.256	4.319	4.09	4.289
10	2.979	3.058	3.026	2.845	4.088	4	4	4.239
15	2.750	2.889	2.972	2.554	3.879	3.845	3.814	4.168
20	2.472	2.416	2.585	2.253	3.345	3.508	3.712	3.878
25	2.281	2.205	2.481	2.076	3	2.976	3.681	3.475
30	2.149	2.190	2.227	1.533	2.576	2.189	3.486	3.3
35	1.425	1.833	1.597	0.904	1.647	-	3.1	3.008
40	-	1.095	1.300	-	1.142	-	2.746	2.989

ACTA SCIENTIAE

ISSN: 2178-7727

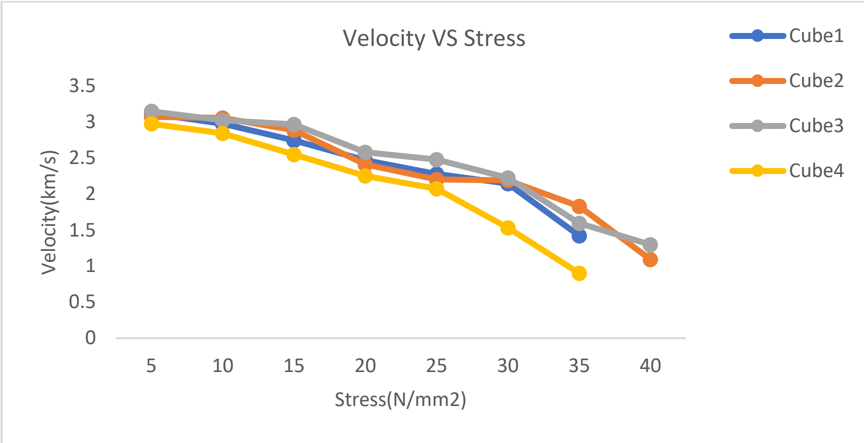

Fig. 9. Velocity versus stress graph of M25, measured using Transducer-1

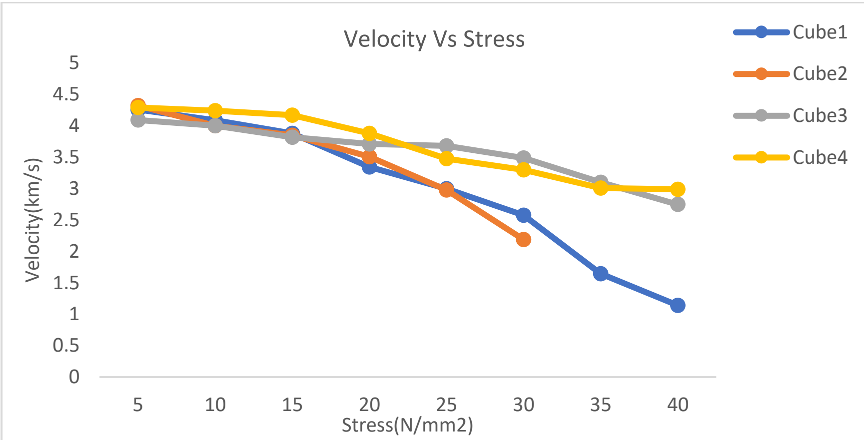

Fig. 10. Velocity versus stress graph of M25, measured using Transducer-2

Table 11. Values of UPV corresponding to M30 concrete

Stress(N/mm^2)	Velocity (km/s)							
	Transducer-1 (28mm dia)				Transducer-2 (49.7mm dia)			
	Cube 1	Cube 2	Cube 3	Cube 4	Cube 1	Cube 2	Cube 3	Cube 4
5	2.934	3.155	3.201	3.002	4.324	4.463	4.131	4.312
10	2.719	3.086	2.989	2.865	4.167	4.098	4.105	4.288
15	2.612	2.869	2.917	2.601	3.913	3.877	3.902	4.134
20	2.489	2.561	2.724	3.087	3.437	3.619	3.812	3.912
25	2.349	2.301	2.514	2.402	3.255	3.215	3.766	3.655
30	2.011	2.273	2.305	1.775	2.711	2.411	3.509	3.498
35	1.602	1.981	1.865	1.018	1.867	1.916	3.166	3.178
40	1.363	-	1.412	-	-	-	-	-

ISSN: 2178-7727

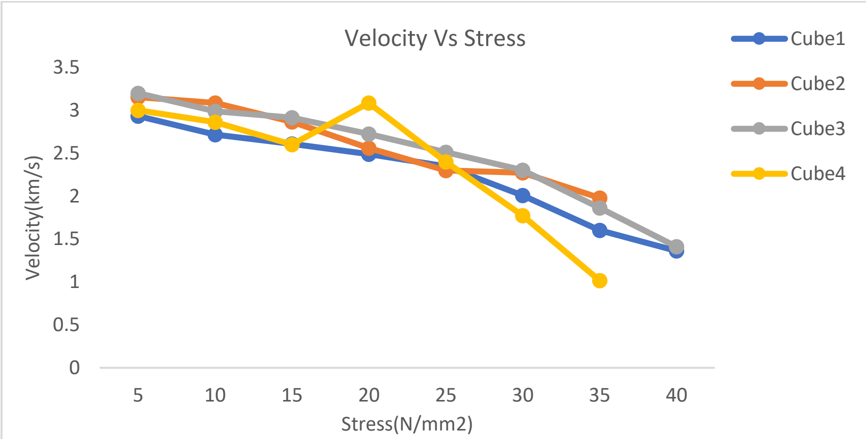

Fig. 11. Velocity versus stress graph of M30, measured using Transducer-1

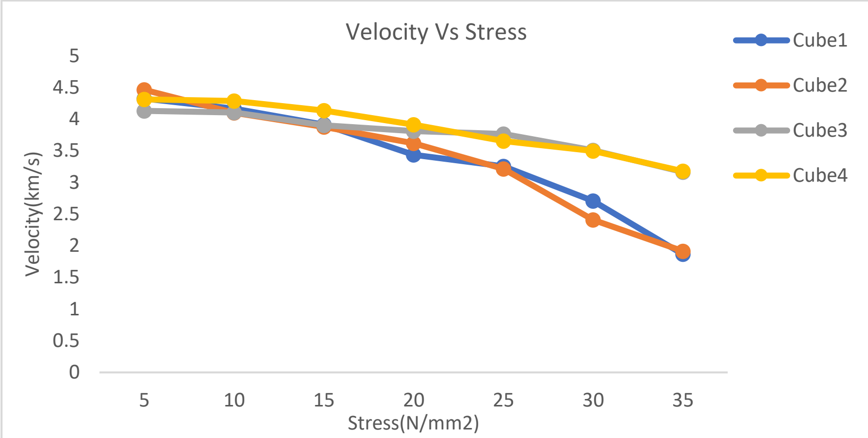

Fig. 12. Velocity versus stress graph of M30, measured using Transducer-2

Table 12. Values of UPV corresponding to M35 concrete

Stress(N/mm^2)	Velocity (km/s)							
	Transducer-1 (28mm dia)				Transducer-2 (49.7mm dia)			
Stress	Cube 1	Cube 2	Cube 3	Cube 4	Cube 1	Cube 2	Cube 3	Cube 4
5	3.126	3.137	2.933	3.040	4.4	4.298	4.015	4.176
10	2.929	2.828	2.826	2.980	4.304	4.165	3.609	4.083
15	2.814	2.667	2.667	2.925	4.201	3.964	3.235	3.971
20	2.667	2.306	2.256	2.843	4.065	3.8	2.807	3.824
25	2.585	2.146	2.158	2.660	3.845	3.741	2.611	3.754
30	2.516	1.668	1.941	2.561	3.7	3.6	2.589	3.621
35	2.283	1.452	-	2.146	3.515	3.456	2.499	3.324
40	2.057	1.124	-	1.884	2.819	-	2.084	3.185
45	-	0.967	-	-	2.981	-	-	-

ISSN: 2178-7727

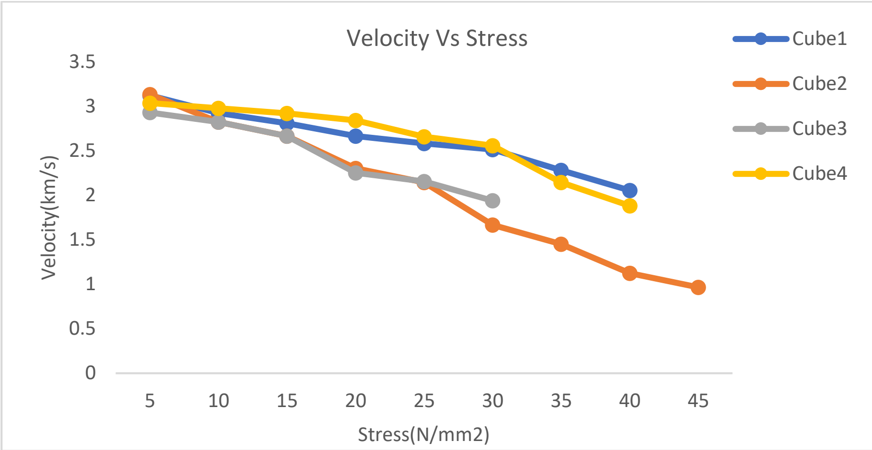

Fig. 13. Velocity versus stress graph of M35, measured using Transducer-1

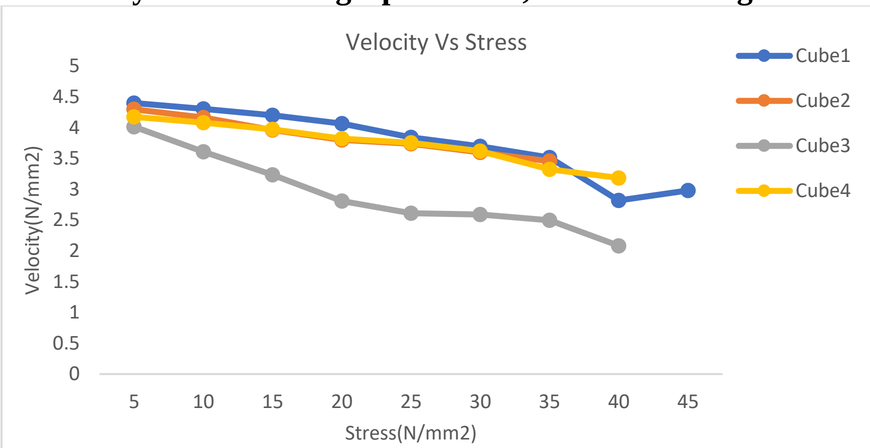

Fig. 14. Velocity versus stress graph of M35, measured using Transducer-2

Table 13. Values of UPV corresponding to M40 concrete

Stress (N/mm^2)	Velocity (km/s)							
	Transducer-1 (28mm dia)				Transducer-2 (49.7mm dia)			
stress	Cube 1	Cube 2	Cube 3	Cube 4	Cube 1	Cube 2	Cube 3	Cube 4
5	3.121	3.159	2.920	3.187	4.498	4.275	4.589	4.251
10	3.058	3.023	2.838	3.035	4.205	4.016	4.389	4.208
15	2.735	2.978	2.663	2.984	4.182	3.952	3.957	4.121
20	2.616	2.840	2.465	2.91	4.05	3.8	3.675	4.105
25	2.318	2.441	2.344	2.741	4.001	3.659	3.145	4.09
30	2.156	2.19	2.263	2.556	3.888	3.392	2.876	3.984
35	1.969	1.825	2.077	2.458	3.854	2.946	2.472	3.854
40	1.711	1.380	1.610	2.190	3.412	2.1	2.1	3.604
45	1.475	-	1.387	1.827	3.098	-	1.742	3.458
50	-	-	-	1.577	2.875	-	1.416	-

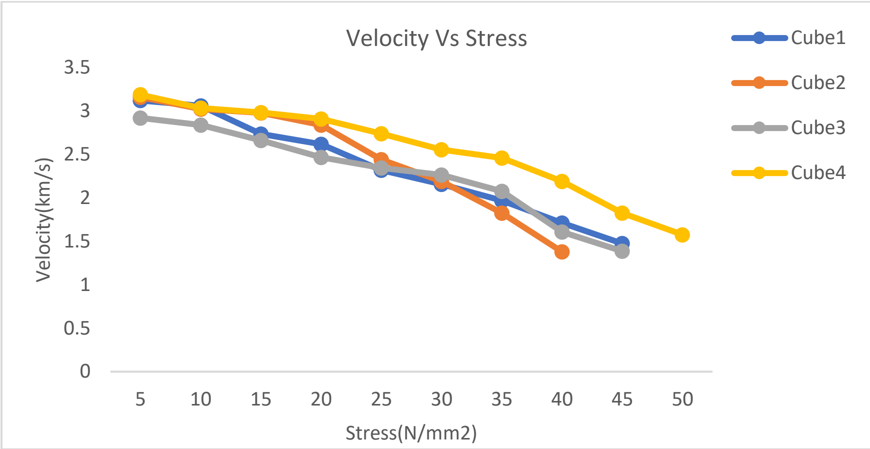

Fig. 15. Velocity versus stress graph of M40, measured using Transducer-1

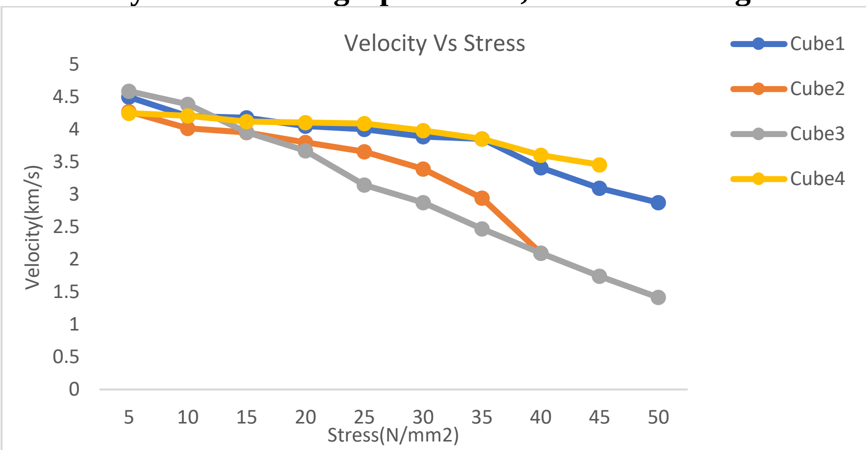

Fig. 16. Velocity versus stress graph of M40, measured using Transducer-2

Table 14. Values of UPV corresponding to M45 concrete

Stress(N/m m^2)	Velocity (km/s)							
	Transducer-1 (28mm dia)				Transducer-2 (49.7mm dia)			
Stress	Cube 1	Cube 2	Cube 3	Cube 4	Cube 1	Cube 2	Cube 3	cube 4
5	3.246	3.148	3.139	3.124	4.345	4.297	4.318	4.413
10	3.169	2.912	3.072	3.019	4.108	4.258	4.256	4.219
15	3.023	2.733	3.034	2.774	3.821	4.219	4.2	4.137
20	2.926	2.555	2.860	2.547	3.384	4.109	4.141	3.8
25	2.692	2.441	2.733	2.171	3.102	4.087	4.111	3.724
30	2.536	2.319	2.476	1.793	2.857	3.872	3.751	3.542
35	2.327	2.036	2.29	1.538	2.489	3.542	3.512	3.175
40	2.004	1.860	2.056	1.362	2.175	3.245	3.108	2.948
45	1.865	1.730	1.808	-	1.746	2.946	2.948	2.486
50	1.593	1.460	1.319	-	-	2.451	-	1.998
55	1.344	-	-	-	-	2.008	-	1.458

ISSN: 2178-7727

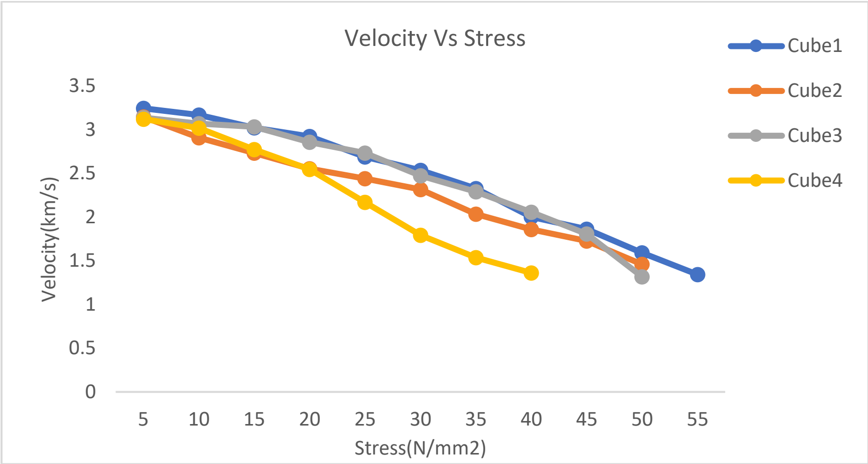

Fig. 17. Velocity versus stress graph of M45, measured using Transducer-1

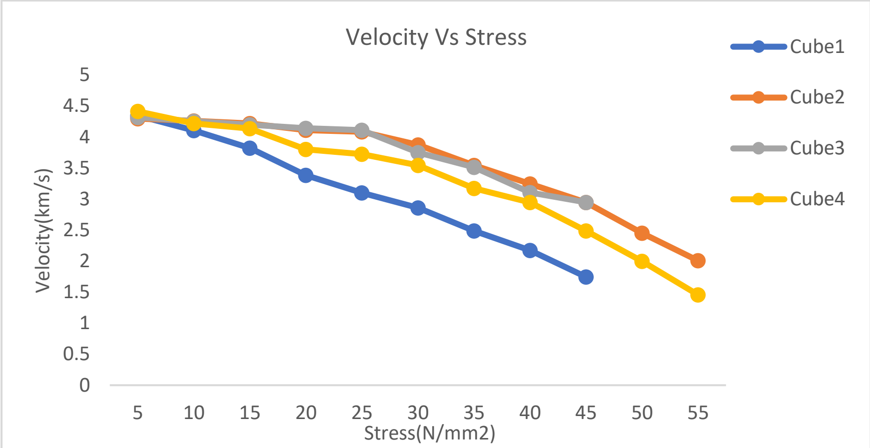

Fig. 18. Velocity versus stress graph of M45, measured using Transducer-2

DISCUSSION

Inverse Correlation between Stress and UPV

The experimental results demonstrated a consistent inverse relationship between compressive stress and Ultrasonic Pulse Velocity (UPV) across all concrete grades (M10–M45). Transducer 2 (49.7 mm diameter) consistently recorded higher baseline UPV values than Transducer 1 (28 mm diameter), attributed to its larger contact area and reduced near-field distortions. For instance, M45 concrete exhibited initial UPV values of 3.12–3.25 km/s (Transducer 1) compared to 4.29–4.41 km/s (Transducer 2) at 5 N/mm². Under progressive loading, Transducer 1 showed steeper velocity declines in high-strength grades (e.g., M45: 59% drop for Transducer 1 vs. 54% drop for Transducer 2 at 50 N/mm²), reflecting its sensitivity to localized micro-cracking. High-grade concrete maintained higher UPV under stress (e.g., M45: Transducer 2 declined from 4.41 km/s to 1.46 km/s at 55 N/mm²) compared to low-grade mixes (e.g., M10: Transducer 2 declined from 4.19 km/s to 1.60 km/s at 30 N/mm²), owing to its lower porosity and superior aggregate-cement bonding, which delayed measurable UPV reductions until advanced loading stages (>80% ultimate stress).

Stress Thresholds for Significant Velocity Decline

In low-grade concrete (M10–M25), Transducer 1 detected abrupt UPV losses earlier (e.g., M10: 3.01 km/s at 5 N/mm² to 0.80 km/s at 30 N/mm²), while Transducer 2 showed gradual declines (e.g., M10: 4.19 km/s to 1.60 km/s), highlighting the smaller transducer's sensitivity to surface-level cracks in porous media. Conversely, high-grade concrete (M35–M45) retained measurable UPV even at extreme stresses with Transducer 2 (e.g., M45: 2.01 km/s at 55 N/mm²), whereas Transducer 1 values collapsed earlier (e.g., M45: 1.34 km/s at 55 N/mm²), emphasizing the larger transducer's ability to average bulk properties and detect residual structural integrity.

ISSN: 2178-7727

Variability in UPV Measurements

Transducer 1 exhibited greater variability at higher stresses (e.g., M15 at 35 N/mm²: 0.87–1.50 km/s vs. Transducer 2: 1.57–2.85 km/s), likely due to localized crack interactions in heterogeneous regions. Missing data ("–") at critical stresses (e.g., M30 Transducer 1 at 40 N/mm²) correlated with specimen failure, observed more frequently in low-grade mixes. Transducer 2 demonstrated narrower data spreads in high-strength grades (e.g., M40 at 40 N/mm²: 3.41–3.60 km/s vs. Transducer 1: 1.38–2.19 km/s), underscoring its robustness in dense concrete.

Grade-Specific Insights

Lower grades (M10–M20): Transducer 1 captured rapid UPV declines (e.g., M10: 3.06 → 0.80 km/s) due to early micro-crack propagation, while Transducer 2 revealed delayed degradation (e.g., M20: 3.85 km/s at 30 N/mm²), bypassing surface porosity. Anomalies such as M20 Cube 4 (Transducer 2: velocity increase at 20 N/mm²) suggested localized compaction undetected by Transducer 1.

Mid-range grades (M25–M35): Transducer 1 identified critical stress thresholds (e.g., M25 at 35 N/mm²: 0.90–3.01 km/s), while Transducer 2 maintained stable readings (e.g., M30 at 25 N/mm²: 3.00–3.98 km/s), reflecting balanced microstructural integrity.

Higher grades (M40–M45): Transducer 2 demonstrated superior durability tracking (e.g., M45: 4.41 → 1.46 km/s at 55 N/mm²), whereas Transducer 1 signalled catastrophic failure earlier (e.g., M45: 3.25 → 1.34 km/s). Non-linear decay in M40 (Transducer 2: 3.85 → 3.46 km/s at 45 N/mm²) indicated progressive internal damage rather than abrupt collapse.

Practical Implications

The 28 mm transducer is optimal for early crack detection in high-strength concrete (e.g., M45), while the 49.7 mm probe is preferred for bulk integrity evaluation in low-strength or porous mixes (e.g., M10–M20). Critical failure thresholds were identified as UPV <1.5 km/s (Transducer 1) and <2.0 km/s (Transducer 2) for high-strength grades.

CONCLUSION

The experimental investigation reveals an inverse correlation between compressive stress and Ultrasonic Pulse Velocity (UPV) in concrete, driven by micro-crack formation disrupting wave transmission. High-grade concrete (M45) showed higher initial UPV (Transducer 1: 3.12–3.25 km/s; Transducer 2: 4.29–4.41 km/s) than low-grade mixes (e.g., M10), owing to its dense microstructure and strong aggregate-cement bonding. The 28 mm transducer detected localized micro-cracking through abrupt UPV drops (>50% at critical stresses), whereas the 49.7 mm transducer, averaging signals over a wider area, maintained stable readings in porous media (e.g., M45: 1.46 km/s at 55 N/mm²). These results confirm UPV's reliability for non-destructive residual strength assessment, with transducer choice (28 mm for early cracking, 49.7 mm for bulk integrity) dependent on material grade and damage stage. A dual-transducer strategy enhances structural monitoring by pairing early crack detection with robust bulk evaluation during progressive failure. Integrating UPV data with mechanical models could refine failure predictions for critical infrastructure under complex loads. Standardizing grade-specific calibration curves for transducers would improve field accuracy, enabling precise residual strength mapping in applications ranging from bridges to prefabricated elements. This approach advances structural health monitoring by aligning sensor capabilities with material behaviour, ensuring targeted damage diagnosis and longevity in diverse concrete systems.

NEW METHODOLOGY

This section details a rigorous methodology to isolate stress-induced effects on Ultrasonic Pulse Velocity (UPV) using two transducers of distinct geometries (**Transducer 1**: 28 mm diameter, 150 kHz; **Transducer 2**: 49.7 mm diameter, 54 kHz). The approach integrates transducer-specific calibration, empirical stress factors, and statistical validation to enhance diagnostic accuracy in concrete structural health monitoring.

ISSN: 2178-7727

Definitions and Parameters

1. **Transducer Specific Correct Velocity (V_{1t})**:
The baseline UPV of unstressed concrete for Transducer t (t=1,2), measured under laboratory-controlled, stress-free conditions. V_{1t} reflects intrinsic material properties (e.g., density, porosity, compressive strength) and accounts for transducer geometry and frequency.
Example: V_{11}=3.25±0.12 km/s (M45, Transducer 1), V_{12}=4.41±0.15 km/*v* (M45, Transducer
2 **Stress Factor** (SF_t):
A dimensionless attenuation coefficient for Transducer t, defined as:

$$SF_t = \frac{V2_t}{V1_t} \quad (1)$$

where V_{2t} is the UPV measured under applied stress (σ). SF_t is derived empirically for each concrete grade (M10–M45) and transducers.

Procedure for UPV Correction

Step 1: Transducer Selection

Transducer 1 (28 mm): Optimal for high-strength concrete (M35–M45) to detect localized micro-cracks (high-frequency sensitivity).
Transducer 2 (49.7 mm): Preferred for low-strength (M10–M25) or porous concrete to assess bulk integrity (low-frequency penetration).

Step 2: Specimen Preparation

Prepare 64 cubic specimens (150 mm × 150 mm × 150 mm) across eight grades (M10–M45), cured for 28 days under controlled humidity (95% RH) and temperature (20±2°C).
Polish surfaces to ensure uniform transducer coupling (ASTM C597-16 standard).

Step 3: Baseline Velocity Measurement (V_{1t})

Measure V_{1t} in unstressed specimens using a hydraulic testing machine (0 N/mm² load) with a ±0.01 km/s resolution ultrasonic pulse-receiver.
Repeat triplicate measurements per specimen to calculate mean V_{1t}.

Step 4: In Situ UPV Measurement (V_{2t})

Apply axial compressive stress (σ) via a servo-controlled universal testing machine (UTM), incrementally loading specimens (5 N/mm² intervals) until failure.

Record V_{2t} at each stress level using the selected transducer, ensuring consistent coupling pressure (10 kPa) via spring-loaded transducers.

Step 5: Stress Quantification

Calculate applied stress (σ) as:

$$\sigma = \frac{F}{A}, \quad (2)$$

where F is the axial force (kN) and A is the cross-sectional area (22500 mm^2).

Step 6: Stress Factor Calibration

For each grade, plot SF_t vs. σ/σ_{ult} (normalized stress), where σ_{ult} is ultimate compressive strength.

Step 7: Correct Velocity Calculation

Compute stress-corrected UPV (V_{1t}) from in situ V_{2t} and SF_t:

$$V1_t = \frac{V2_t}{SF_t} \quad (3)$$

ISSN: 2178-7727

Step 8: Statistical Validation

Validate results via ANOVA (p<0.05*p*) across 8 specimens per grade, ensuring inter-specimen variability <10% for V_{1t}.

SIGNIFICANCE

This methodology advances non-destructive evaluation (NDE) by decoupling stress effects from material quality. It establishes transducer-specific protocols for accurate residual strength prediction, critical for aging infrastructure assessment. The integration of dual-transducer data mitigates limitations of single-probe UPV systems, enhancing diagnostic reliability in diverse concrete grades.

Funding: No funding was received for this research.

REFERENCES

1. IS 13311 (Part 1):1992-Non-destructive testing of Concrete-Methods of text Pun 1 ultrasonic pulse velocity.
2. IS 456: 2000 Code of Practice for Plain and Reinforced Concrete.
3. Belarbi Hassabu, Mellas Mekki, Rahmani Farid (2017-2018) - The Relation Between Compressive Strength and Ultrasonic Pulse Velocity Concrete with Fiber Exposed to High Temperatures.
4. Mahdi Shariati, Nor Hafizah Ramli-Sulong, Mohammad Mehdi Arabnejad K. H. PayumShafigh and Hamid Sinari [2011]- Assessing the strength of reinforced concrete structures through Ultrasonic Pulse Velocity and Schmidt Rebound Hammer tests.
5. Mohammadreza Harmidian, Mashdi Shariani. M.M. Arabnejad and Hamid Sanses [2011]-Assessment of high strength and light weight aggregate concrete properties using ultrasonic pulse velocity technique.
6. Chong Choot Yeng [2010] -The effect of compressive stress in concrete on ultrasonic pulse velocity.
7. Mouhcine Benaicha, Olivier Jalbaud, Adil Hafidi Alaoui, Yves Burtschell [2015]- Correlation between the mechanical behavior and the ultrasonic velocity of fiber-reinforced concrete.
8. Sandor Popovics, Joseph L. Rose, John S. Popovics, The behavior of ultrasonic pulses in concrete, Cem. Concr. Res. [1990] 259-270.
9. B.S.1881-203, Testing concrete-recommendations for measurement of the velocity of ultrasonic pulses in concrete, British Standards Institution, 1986, p.24.
10. R. Jones, Non-Destructive Testing of Concrete, Cambridge University Press. London, 1962.
11. S. Popovics. J.S. Popovics. A critique of the ultrasonic pulse velocity method for testing concrete, in F. Ansari, S. Sture (Eds.), Non-destructive Testing of Concrete Elements and Structures, Engineering Division of ASCE, San Antonio, Texas, 1992, pp. 94-103.
12. S. Selleck, EN. Landis, M.L. Peterson, S.P. Shah, J.D. Achenbach, Ultrasonic investigation of concrete with distributed damage. ACI Mater. J. 95 (1998) 27-36.
13. T.R. Naik, V.M. Malhotra, The ultrasonic pulse velocity method, in: V.M. Malhotra, N.J. Carino (Eds.), Handbook on Non-destructive Testing of Concrete. CRC Press, Boca Raton, FL, 1991, pp. 169-188.
14. Malhotra. V. M., and Carino N. J. Handbook on Non-destructive Testing of Concrete, CRC Press, Boca Raton, FL, 1991, 343p.
15. Kaplan, M.F. Compressive Strength and Ultrasonic Pulse Velocity Relationships for Concrete in Columns. ACI J., 29(54-37).1958, p. 675.
16. Popovics JS. Ultrasonic testing of concrete structures, Mater Eval 2005:50-5.
17. BS EN12504-4. Testing concrete - Part 4: determination of ultrasonic pulse velocity; 2004.
18. Vishwajeet Surshetwar, Krishna Gattewar, Bhagya Shree Wange, Trupti Gavit, Mr. Ravi Ranade, Mrs. Prital G. Kalasur [2020] - Effect of Compressive Stress on Ultrasonic Pulse Velocity.
19. R. Latif Al-Mufti, A.N. Fried [2012]- The early age non-destructive testing of concrete made with recycled concrete aggregate, Elsevier, Volume 37, pp.379-386.
20. Jain A., Katharia A. Kumar A., Verma Y., Krishna M., (2013), “Combined use of Non-destructive Tests for Assessments of strength of Concrete in Structure". Elsevier, Volume 54, pp.241-251.
21. Ortiz, J.D., Dolati, S.S.K., Malla, P., Mehrabi, A. and Nanni, A., 2024. Nondestructive testing (NDT)

ISSN: 2178-7727

for damage detection in concrete elements with externally bonded fiber-reinforced polymer. Buildings, 14(1), p.246

22. Ottosen, L.M., Kunther, W., Ingeman-Nielsen, T. and Karatosun, S., 2024. Non-Destructive Testing for Documenting Properties of Structural Concrete for Reuse in New Buildings: A Review. Materials, 17(15), p.3814
23. Jayale, V. and Patil, A., 2024, December. Non-destructive test techniques and methods in the assessment of concrete structures a review. In AIP Conference Proceedings (Vol. 3188, No. 1). AIP Publishing.
24. Boccacci, G., Frasca, F., Bertolin, C. and Siani, A.M., 2024. Diagnosis of Historic Reinforced Concrete Buildings: A Literature Review of Non-Destructive Testing (NDT) Techniques. Procedia Structural Integrity, 55, pp.160-167.
25. Wu, W., Li, H., Elghazouli, A.Y. and Wu, Y., 2024. Prediction of axial compressive stresses in ultra-high-performance concrete blocks using non-destructive ultrasonic techniques. Journal of Building Engineering, 95, p.110326.
26. Jain, H. and Patankar, V.H., 2024. Simulations and experimentation of ultrasonic wave propagation and flaw characterisation for underwater concrete structures. Nondestructive Testing and Evaluation, 39(6), pp.1581-1598.
27. Yu, T. and Abazarsa, M., Multiphysical Ndt for Predicting Compressive Strength of Portland Cement Concrete Using Synthetic Aperture Radar, Ultrasonic Testing, and Rebound Hammer. Ultrasonic Testing, and Rebound Hammer.
28. Patel, A.K., 2024. Exploring the Relationship between NDT and DT Techniques in Concrete: Linear and Non-linear Models.